Texture of Crystalline Solids, 1980, Vol. 4, pp. 13-40
0309-7951/80/0401-0013$04.50/0

Printed in the United States of America

SPATIAL ORIENTATION DISTRIBUTION OF CRYSTALLITES IN COLD-ROLLED AND IN ANNEALED SHEETS OF DEEP-DRAWING PHOSPHORUS STEEL

HSUN HU

U.S. Steel Research Laboratory,
Monroeville, PA 15146, U.S.A.

(Received September 9, 1979)

Abstract: The cold-rolling and annealing textures of a deep-drawing phosphorus steel have been studied by the spatial orientation distribution of the crystallites. The characteristics of the orientation distribution functions of the as-cold-rolled and of the annealed sheets were closely examined. The observed features suggest that the annealing texture is originated by microband or transition-band nucleation, followed by the growth of recrystallized grains at the expense of the matrix deformation textures. The crystallite orientation distribution of the annealed sheet of the deep-drawing phosphorus steel is clearly different from that of the annealed sheet of deep-drawing aluminum-killed steels.

INTRODUCTION

It was shown earlier that the addition of phosphorus to low-carbon low-manganese steels substantially improves the deep-drawing capabilities and strength of cold-rolled and annealed sheets.[1] Results of subsequent investigations[2-5] further indicate that these excellent properties of phosphorus steels are not adversely affected by increasing the manganese content up to 0.25 percent,[2] and the carbon content up to 0.05 percent.[3] An additional increase in both the yield and tensile strengths without significantly impairing the drawability and the ductility of the phosphorus steel sheets can be obtained by increasing the silicon content up to about 1.0 percent.[4]

Further increases in yield strength, at some sacrifice of the drawability and ductility, can be achieved through grain refinement[5] by annealing at low temperature or by utilizing a rapid heating and an abbreviated annealing cycle such as the conventional continuous annealing, or by electrical induction annealing with high heating rates. On the other hand, when a

superior drawability rather than a higher strength is desired, the steel can be annealed at an intercritical temperature, for example 780°C (1435°F), which is substantially higher than the normal box-annealing temperature (710°C or 1310°F). All these characteristics apply to vacuum-melted as well as to air-melted phosphorus steels.

In view of the potential versatility and importance of the phosphorus steels, more extensive studies of their deformation and annealing textures, and their anisotropic properties have been conducted. In the present investigation, the spatial-orientation distribution of the crystallites in the as-cold-rolled and in the subsequently annealed specimens were analyzed by using the spherical harmonics method of Roe[6,7] and Bunge.[8,9] The application of Roe's formulation to the orientation-distribution analysis for a grain-oriented electrical steel and a low-carbon aluminum-killed steel was first demonstrated by Morris and Heckler.[10] The use of crystallite orientation distribution function for studying the textures of various metal sheets has become increasing popular in recent years. The present work comprises the first application of this technique to texture analysis for the deep-drawing phosphorus-steel sheets.

MATERIALS AND EXPERIMENTS

Steel Composition and Processing

A previously prepared air-melted low-carbon steel containing approximately 0.07 percent phosphorus was used in the present study. The chemical composition of the steel is given in Table I. The ingot was hot-rolled to a band 3.8 mm (0.15 inch) thick with the finishing pass at 925°C (1700°F), and water-spray-cooled to 620°C (1150°F), then furnace-cooled at a rate of about 40°C (75°F) per hour to simulate the cooling conditions in commercial coils. The hot-rolled band was cleaned by sandblasting and pickling, then cold-rolled 80 percent to 0.8 mm (0.030 inch) thick. Strips suitable for texture determinations for spatial-orientation-distribution analysis were cut from the rolled sheet. Simulated box annealing was conducted in an atmosphere of 15 percent $H_2 + N_2$ by heating at a rate of 20 to 25°C (40 to 50°F) per hour to an intercritical temperature of 780°C (1435°F), holding at 780°C for 20 hours, and furnace-cooling to room temperature.

The Spatial-Orientation-Distribution Analysis

For spatial-orientation-distribution analyses, texture data from three x-ray pole figures of different reflections were first obtained. A composite sampling technique, which was introduced by Meieran[11] and by Lopata and Kula,[12] and later modified by Leber[13] and by Elias and Heckler,[14] was used to determine one complete quadrant of each of the (110), (200), and (211) pole figures by the Schulz reflection technique,[15] using MoK_α radiation and a Siemens texture goniometer. Figure 1 shows these quadrant pole figures of the as-cold-rolled

TABLE I

Chemical Composition of the Air-Melted Phosphorus Steels, Weight Percent

Steel (Air-Melt) 7364-8028		C	Mn	P	S	Si	Cu	Ni	Cr	Al_{Sol}	Al_{total}	N	O_{ppm}
A	T	0.015	0.170	0.067	0.023	0.030	0.017	0.012	0.018	0.009	0.018	0.006	828
	B	0.017	0.170	0.067	0.024	0.032	0.019	0.012	0.020	0.007	0.009	0.005	387

Note: T = top of ingot
B = bottom of ingot

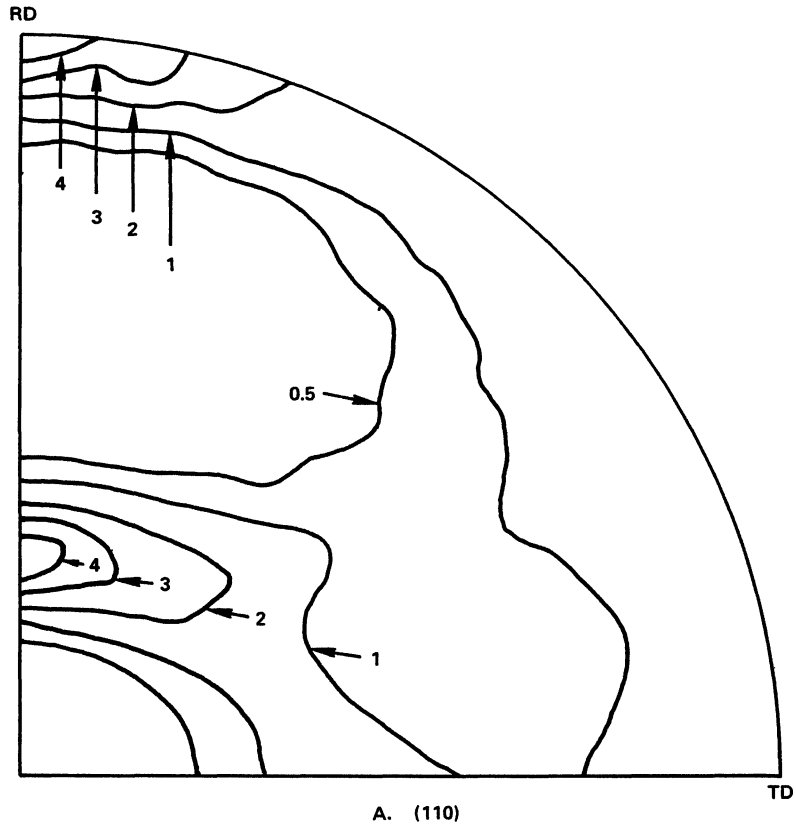

Figure 1A. Pole figure of the as-cold-rolled phosphorus-steel sheet, (110) reflections.

strip, and Figure 2 shows the corresponding quadrant pole figures of the annealed strip. The intensity data of these pole figures were used for spatial-orientation-distribution analyses.

A method for determining the spatial-orientation distribution of the crystallites from several conventional pole figures (the so-called "pole figure inversion") was developed independently by Roe[6] and by Bunge[8] in 1965. The mathematical treatment of the problem and the results obtained by these authors were essentially the same. A set of Eulerian angles is used to define the relationship between the crystallite coordinate system and the specimen, or physical, coordinate system. Following the notations used by Roe,[6] the rotational relationship between these two coordinate systems is illustrated in Figure 3. The rotations are taken in succession in the sequence of ψ-, θ-, and ϕ-rotations as shown. Any crystallite orientation with respect to the physical reference frame can thus be specified by a set of Eulerian angles (ψ, θ, ϕ) in the orientation space. In Figure 4, an example is given for these sequential rotations of $\psi = 60$, $\theta = 54.7$, and $\phi = 45$ degrees in a stereographic projection. The orientation of this crystal is (111)[$1\bar{2}1$] with reference to the specimen coordinate system

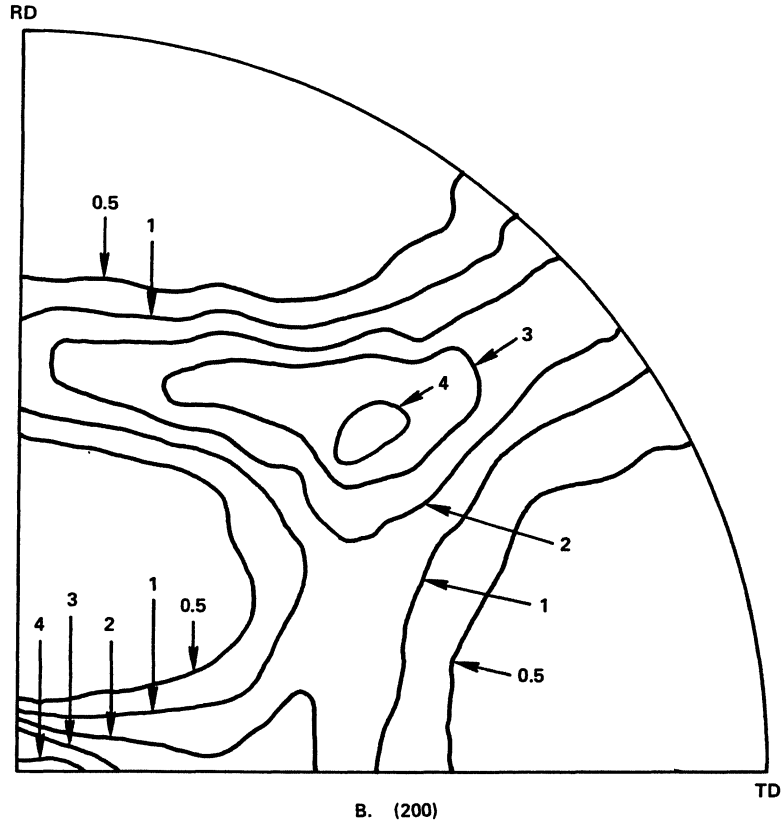

Figure 1B. Pole figure of the as-cold-rolled phosphorus-steel sheet, (200) reflection.

The method developed by Roe[6,7] and by Bunge[8,9] for pole figure inversion actually involves the expansion of the plane-normal orientation distributions (that is, pole figures) in a series of spherical harmonics, and the solution of simultaneous equations relating the coefficients of these harmonics with the coefficients of a series of generalized spherical harmonics. The expansion of this latter series of generalized spherical harmonics forms the crystallite orientation distribution function, which is in the form of

$$w(\psi,\theta,\phi) = \sum_{\ell=0}^{\infty} \sum_{m=-\ell}^{\ell} \sum_{n=-\ell}^{\ell} W_{\ell mn} Z_{\ell mn} (\cos\theta) \exp(-im\psi)\exp(-in\phi) \qquad (1)$$

where the $W_{\ell mn}$ are the coefficients of the series, and the $Z_{\ell mn}(\cos\theta)$ are the augmented Jacobi polynomials. Thus, the coefficients of the orientation distribution function, $W_{\ell mn}$, are directly related to the coefficients of the plane-normal distribution (or pole figure) expansion.

Considerations of specimen or physical symmetry of rolled sheet, and of crystallographic symmetry of the cubic system

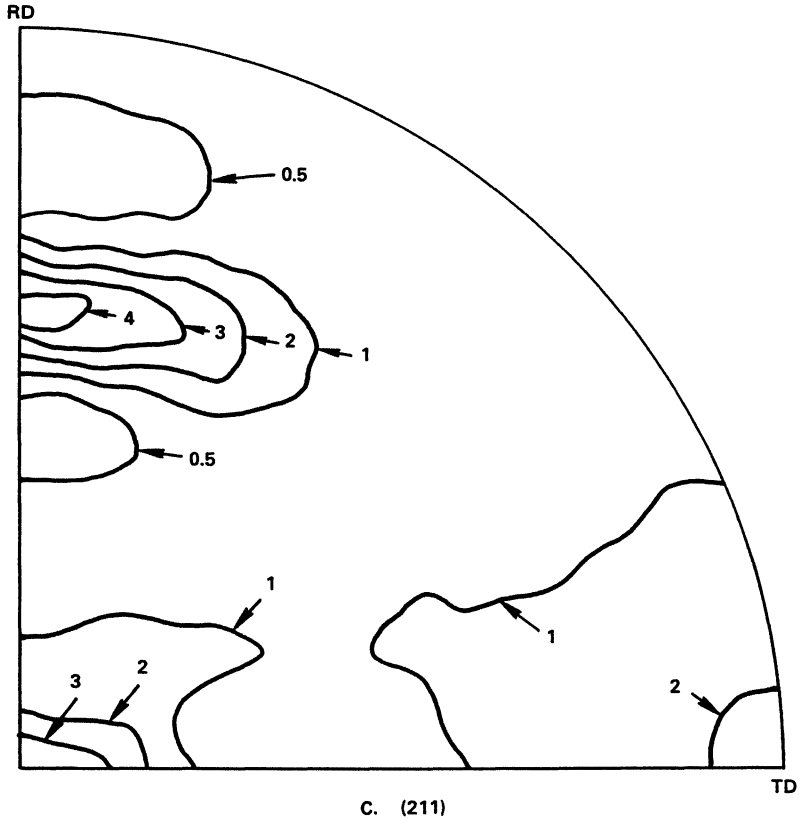

Figure 1C. Pole figure of the as-cold-rolled phosphorus-steel sheet, (211) reflection.

impose restrictions on the series and coefficients. The ℓ and m are restricted to even values, and n is restricted to 4k, where k = 0,1,3...etc. The Jacobi polynomials, $Z_{\ell mn}$, have been derived for the orthotropic physical symmetry (sheet specimens) and cubic crystallographic symmetry in multiple angle form by Morris and Heckler.[10] Numerical values of $Z_{\ell mn}$ up to ℓ = 16 have also been provided by these authors in tabular form. A computer program for calculation of $Z_{\ell mn}$, up to ℓ = 32, was recently published by Morris.[16] Improvements in the computing techniques for data processing in spatial orientation distribution analysis have been discussed by Jura and Pospiech[17] recently.

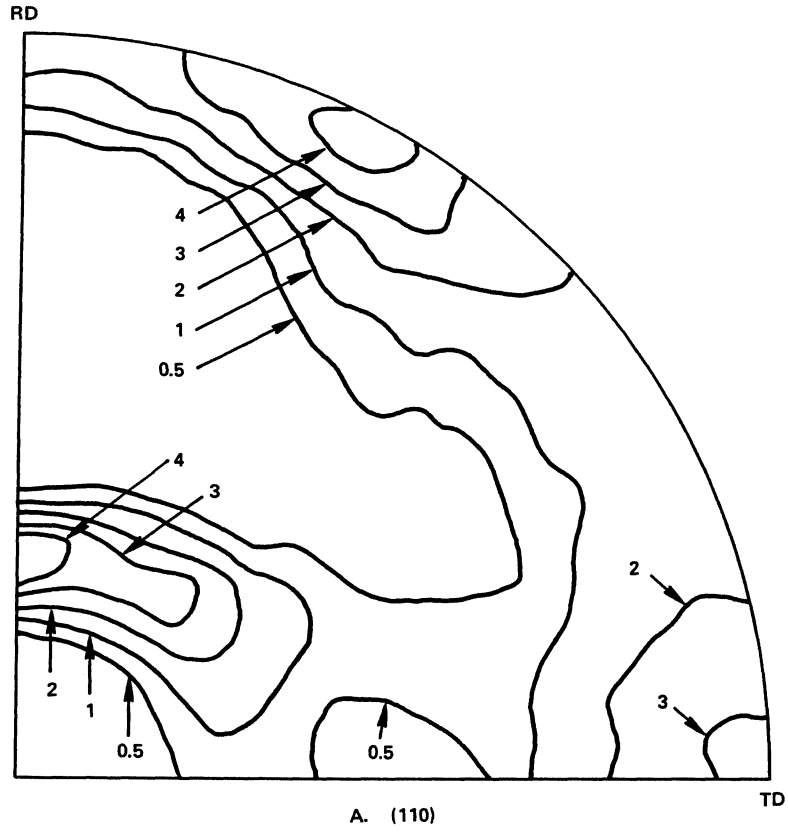

Figure 2A. Pole figure of the annealed phosphorus-steel sheet, (110) reflection.

RESULTS AND DISCUSSION

Orientation Distribution of Crystallites in the Cold-Rolled Sheet

The spatial-orientation distribution of the crystallites can best be represented by a three-dimensional model, or diagram, with the Eulerian angles (ψ,θ,ϕ) as the orthogonal coordinates. Bunge, et al.[18] plotted the intensity contour lines of the orientation-distribution function for constant-ϕ sections on plexiglass slabs, and stacked these slabs one upon another to form a three-dimensional model. The orientation distribution of the crystallites in the Eulerian space can thus be visualized directly. However, since much work is involved in constructing such models, most authors still prefer the use of a series of two-dimensional plots of constant-ϕ, or less frequently, constant-ψ, sections. The crystallite-orientation distribution in Eulerian space can then be visualized by placing the sections one upon another, and by picturing that the iso-intensity contour lines of neighboring

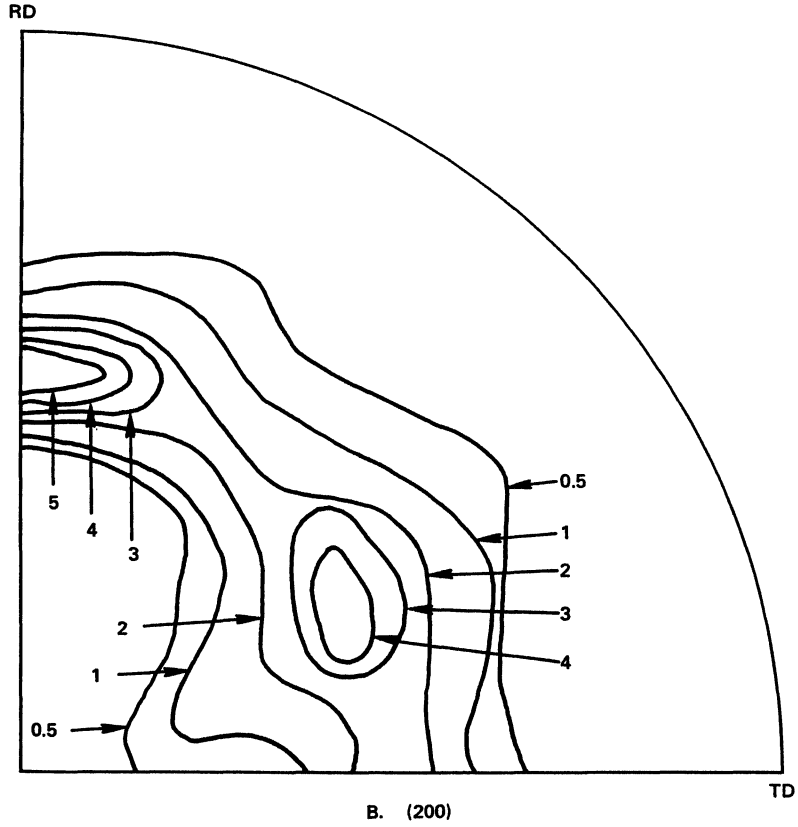

Figure 2B. Pole figure of the annealed phosphorus-steel sheet, (200) reflection.

sections are being connected into iso-intensity surfaces. Figure 5 shows the spatial-orientation distribution of crystallites in the as-cold-rolled sheet in constant-ϕ sections.

The distribution function $w(\psi,\theta,\phi)$ shown as an infinite series in Eq. (1) was truncated at $\ell = 16$. The truncation error can be estimated and was discussed by Roe,[6] Bunge,[9] Morris and Heckler,[10] and others.[19] In general, for truncation at a given order of ℓ, the magnitude of truncation error depends on the sharpness of the texture. For very sharp and strong textures truncation should be employed at high values of ℓ to minimize the error due to truncation. However, experimental errors in pole-figure determination may render a high-order truncation meaningless, when the experimental errors of the pole-figure data are greater than that due to truncation.

The constant-ϕ sections of the spatial-orientation distribution shown in Figure 5 were taken at 5-degree intervals from $\phi = 0$ to $\phi = 90$ degrees. The $\phi = 90$ section was omitted for presentation, because it was the same as the $\phi = 0$ section. As these sequential sections show, the crystallites in the as-cold-rolled steel sheet are oriented crystallographically by clustering in the Eulerian space in tubular or banded forms. For sheet textures of cubic metals, most of the "ideal

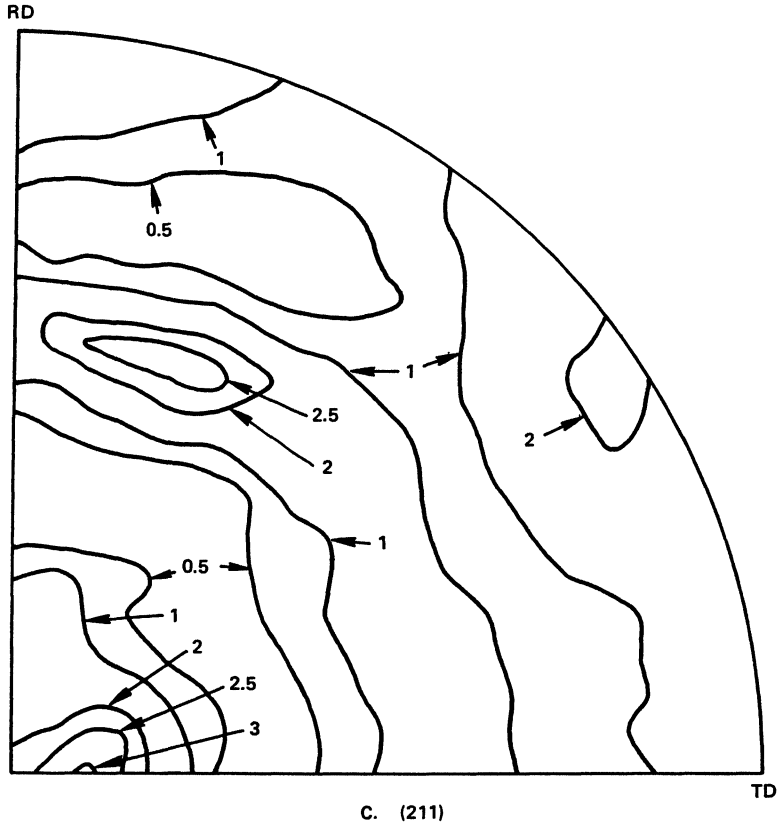

Figure 2C. Pole figure of the annealed phosphorus-steel sheet, (211) reflection.

orientations" can be identified in the $\phi = 45$ section, as shown in Figure 6. Comparing the $\phi = 45$ section of Figure 5 with Figure 6 shows that the cold-rolling texture of the present steel sheet contains a very strong $(\bar{1}12)[\bar{1}\bar{1}0]$ component, a fairly strong $(001)[1\bar{1}0]$ component, and a prominent fiber texture of $[111]$ in the normal direction (ND) extending continuously from $(\bar{1}11)[\bar{1}\bar{1}0]$ to $(\bar{1}11)[1\bar{1}\bar{2}]$. Orientation spread around the ideal positions having a $[\bar{1}\bar{1}0]$ direction in the rolling direction (RD) extends from $(001)[\bar{1}\bar{1}0]$ to slightly beyond $(\bar{3}31)[\bar{1}\bar{1}0]$. These characteristics are typical of the rolling textures of iron and steels.

The ideal orientations shown in Figure 6 or any crystallite orientation in the Eulerian space that can be expressed in the form (hkl)[uvw], where (hkl) refers to the crystallographic plane lying parallel to the rolling plane of the sheet, and [uvw] to the crystallographic direction in that plane parallel to the rolling direction, can be obtained by simple calculations from the Eulerian angles. The elements of the transformation matrix formulated by Roe[6] for the rotation of the coordinate axes by the Eulerian angles can be used for this purpose. In that matrix (Equation 4 of Roe[6]), the

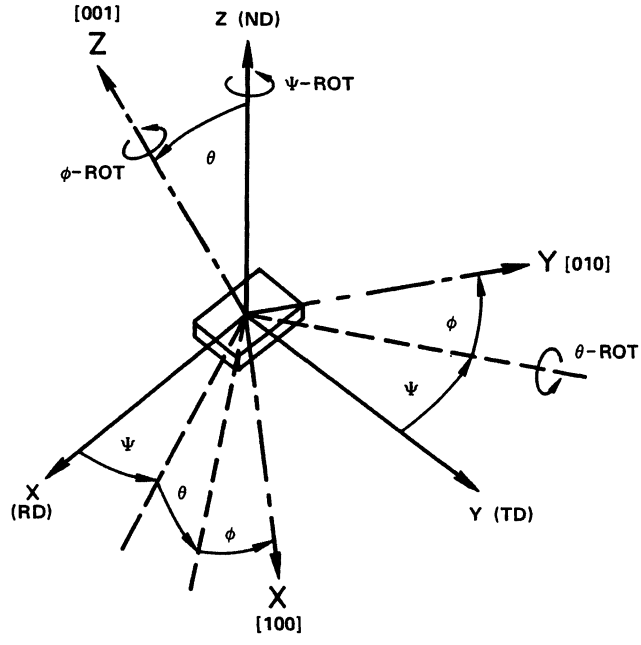

Figure 3. Diagram illustrating the relationship between the crystal coordinate system XYZ and the specimen or physical coordinate system xyz by the Eulerian angles ψ,θ,ϕ through successive rotations in the sequence of ψ-, θ-, and ϕ-rotations.

elements in the first column give the indices of the rolling direction; those in the second column, indices of the transverse direction; and those in the third column, indices of the normal direction on the rolling plane (since for the cubic system, the indices for the plane and its normal direction are the same). Thus, for (hkl) of the rolling plane,

$$h = - \sin\theta \cos\phi$$

$$k = \sin\theta \sin\phi$$

$$\ell = \cos\theta \ ;$$

and for [uvw] of the rolling direction,

$$u = \cos\psi \cos\theta \cos\phi - \sin\psi \sin\phi$$

$$v = - \cos\psi \cos\theta \sin\phi - \sin\psi \cos\theta$$

$$w = \cos\psi \sin\theta .$$

To facilitate the analysis of crystallite-orientation-distribution plots, Davies, et al.[20] have prepared a set of charts for various constant-ϕ sections. These charts contain all the ideal orientations (hkl)[uvw] for cubic materials formed by permuting the Miller's indices through 3 to -3. Like standard projections, which are frequently used for

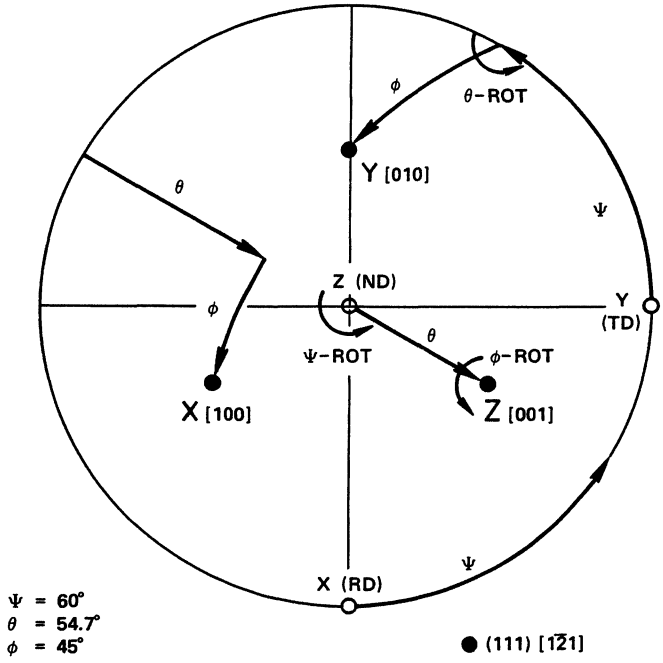

Figure 4. Stereographic projection showing the orientation of a crystal as defined by a set of Eulerian angles in relation to the specimen coordinate system.

identifying texture components in conventional pole figures, these charts can be used for similar purposes in dealing with spatial-orientation-distribution plots.

The spatial-orientation distribution as shown by the constant-ϕ sections in Figure 5 indicates that the intensity, or the orientation density, of the prominent [111] fiber texture in ND has its highest values at the core of the "tube," which extends in a direction approximately parallel to the ψ-axis in the Eulerian space. Hence the cross-sectional details of the "tube" will be better revealed in constant-ψ sections of the spatial-orientation-distribution plots. These are shown in Figure 7 at 5-degree intervals of ψ. The ψ = 5 section was not shown in the illustration, because the plot was nearly the same as the ψ = 0 section.

As shown by the sequence of constant-ψ sections, the texture of the as-cold-rolled phosphorus-steel sheet can be considered as composed of two principal branches or components: the (111) fiber component A and the (001) component B. The orientation of the component A at the core of the tube varies along the length of the tube (the "skeleton line" described by Bunge[9]).

The orientation variations along the skeleton line of component A and of component B are shown in Figure 8 in a stereographic projection. The rolling plane (or normal direction) of component A varies within a narrow range around ($\bar{1}11$). The numbers 1, 2, 3, ..., 19 refer to the sequence of

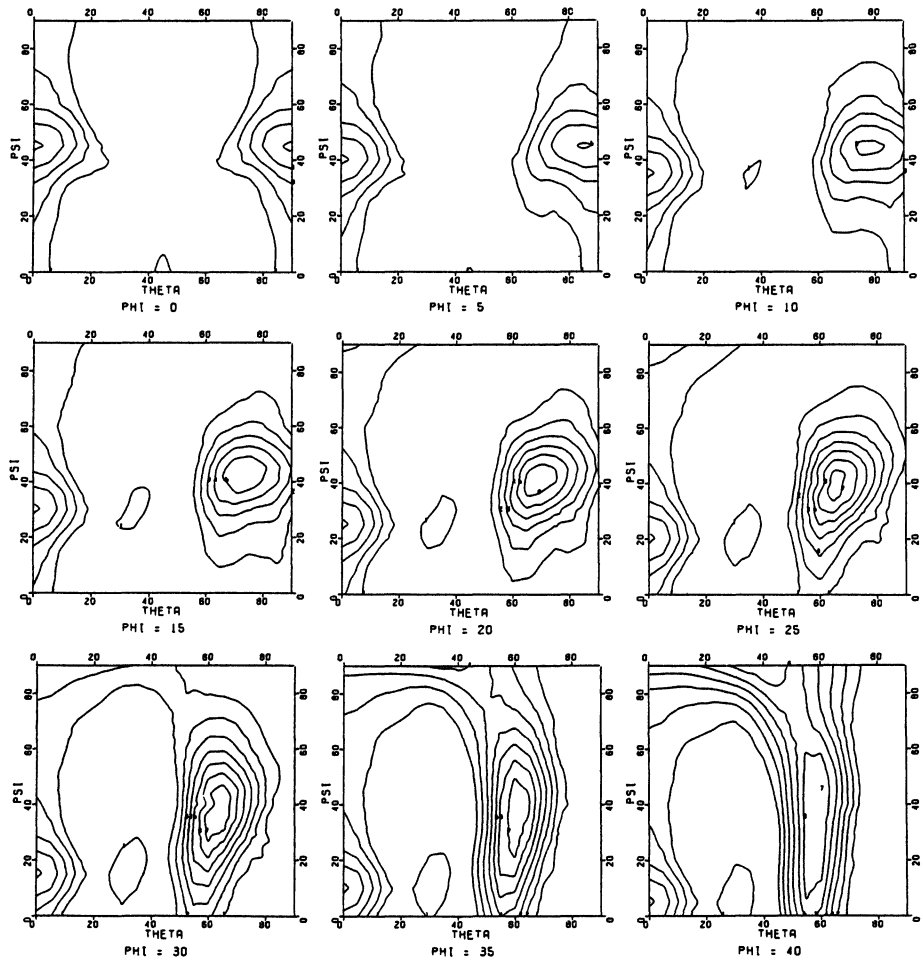

Figure 5. Spatial orientation distribution of crystallites in the as-cold-rolled phosphorus-steel sheet psi (ψ) vs theta (θ) at constant phi (ϕ) sections. Orientation density contours at 1, 2, 3 ... times random units.

constant-ψ sections at 5-degree intervals from $\psi = 0$ to $\psi = 90$, Figure 7. As shown, the rolling-plane orientation oscillates between $(\bar{1}11)$ and nearly $(\bar{2}11)$, then from $(\bar{1}11)$ toward $(\bar{1}12)$, whereas the rolling direction changes approximately along the $(\bar{1}11)$ great circle from $[1\bar{1}2]$ through $[0\bar{1}1]$ and $[\bar{1}\bar{2}1]$ to $[\bar{1}\bar{1}0]$. The orientation of component B is much more stable than that of component A. The rolling plane of component B remains at (001), and the rolling direction can be described as $[1\bar{1}0]$ and $[\bar{1}\bar{1}0]$, which are equivalent crystallographically and physically with respect to the specimen coordinate system.

The intensity of orientation-density variations along the skeleton lines of the texture components are shown in Figure 9. The orientation density of the fiber component A varies significantly from a minimum at the $(\bar{1}11)[1\bar{1}2]$ and

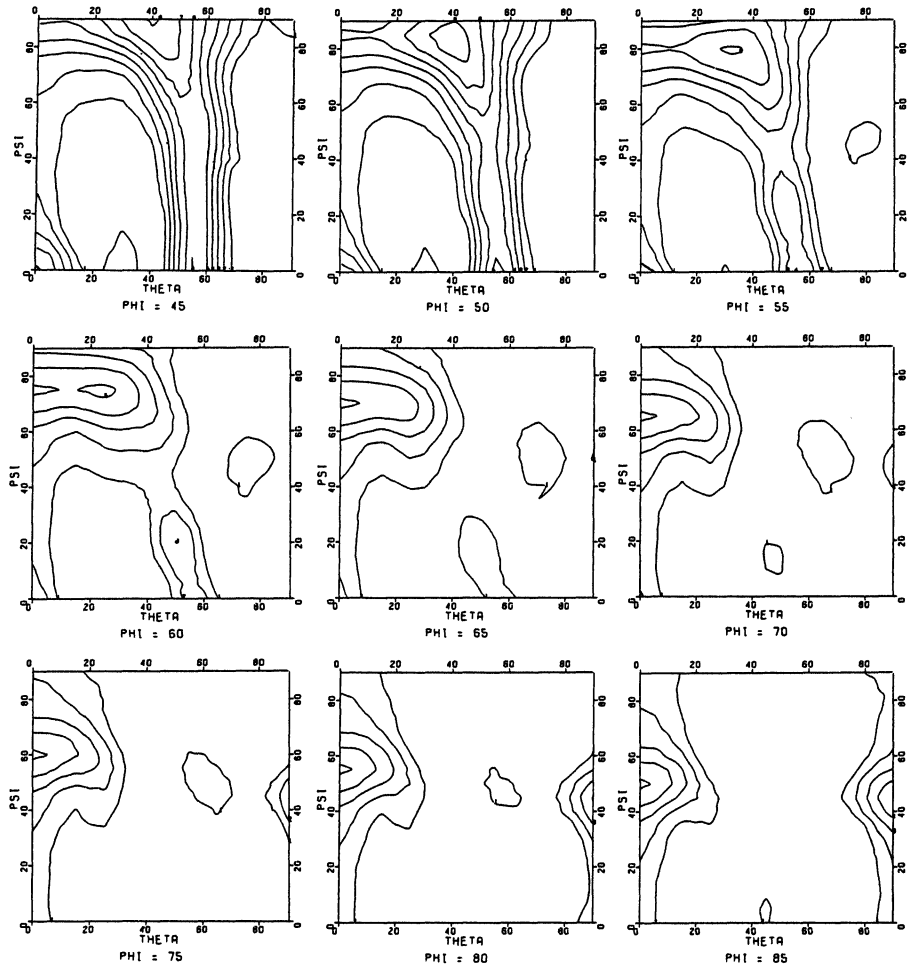

Figure 5. (continued)

$(\bar{1}\bar{1}1)[\bar{1}\bar{2}1]$ orientations to a maximum at approximately $(\bar{2}11)$ $[0\bar{1}1]$ and $(\bar{5}58)[\bar{1}\bar{1}0]$ orientation. The component B, which can be described as $(001)[1\bar{1}0]$, has a uniform orientation density along the entire skeleton line of the tube.

Orientation Distribution of Crystallites in the Annealed Sheet

The spatial-orientation distribution of crystallites in the annealed (780°C for 20 hours) phosphorus-steel sheet was analyzed similarly. Figure 10 shows the orientation-distribution plots in constant-ϕ sections. It is immediately evident that the annealing texture is considerably stronger than the rolling texture (Figure 5), as shown particularly by the ϕ = 30 to 55 sections. The nature of the texture in terms of ideal orientations can be identified by comparing the ϕ = 45 section with Figure 6. As may be recognized readily, the annealing texture of the phosphorus-steel sheet is predominantly the [111] fiber in the normal direction of the sheet, with maximum

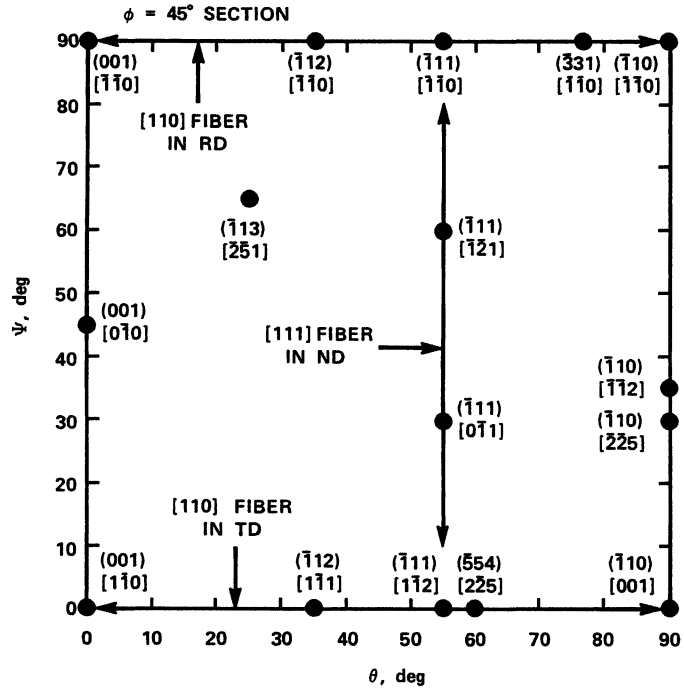

Figure 6. Ideal orientations in the ϕ = 45 section of the spatial-orientation distribution.

orientation density at $(\bar{1}11)[\bar{1}\bar{2}1]$ and $(\bar{1}11)[1\bar{1}2]$ positions. As in the orientation distribution of crystallites in the cold-rolled sheet (Figure 5), the [111] fiber extends in a direction approximately parallel to the ψ-axis in the Eulerian space.

To reveal the cross-sectional details of the orientation-distribution tube of the [111] fiber texture, constant-ψ sections of the spatial orientation distribution function were obtained, as shown in Figure 11. It can be seen that in the sequence of the constant-ψ sections, one or two minor texture components were developed. If the major fiber texture is designated as component A and the minor ones as components B and C, the orientation variations of these components are shown in Figure 12. As in Figure 8, the numbers 1, 2, 3, ... 19 refer to the sequence of constant-ψ sections from ψ = 0 to 90 at 5-degree intervals. The major component A has its rolling plane oriented near and around $(\bar{1}11)$, and its rolling direction ranged from near $[1\bar{1}2]$, through $[0\bar{1}1]$ and $[\bar{1}\bar{2}1]$ to $[\bar{1}\bar{1}0]$. This range of orientations is essentially the same as that in the cold-rolled sheet. However, as will be seen later, the maximum orientation densities occur at different regions within the range of the fiber-texture orientations.

The minor components B and C have their rolling-plane orientations near $(\bar{3}11)$ and $(\bar{1}13)$, respectively, and their rolling directions somewhat deviated from that of component A, or the $(\bar{1}11)$ great circle. The $(\bar{3}11)$ and $(\bar{1}13)$ are

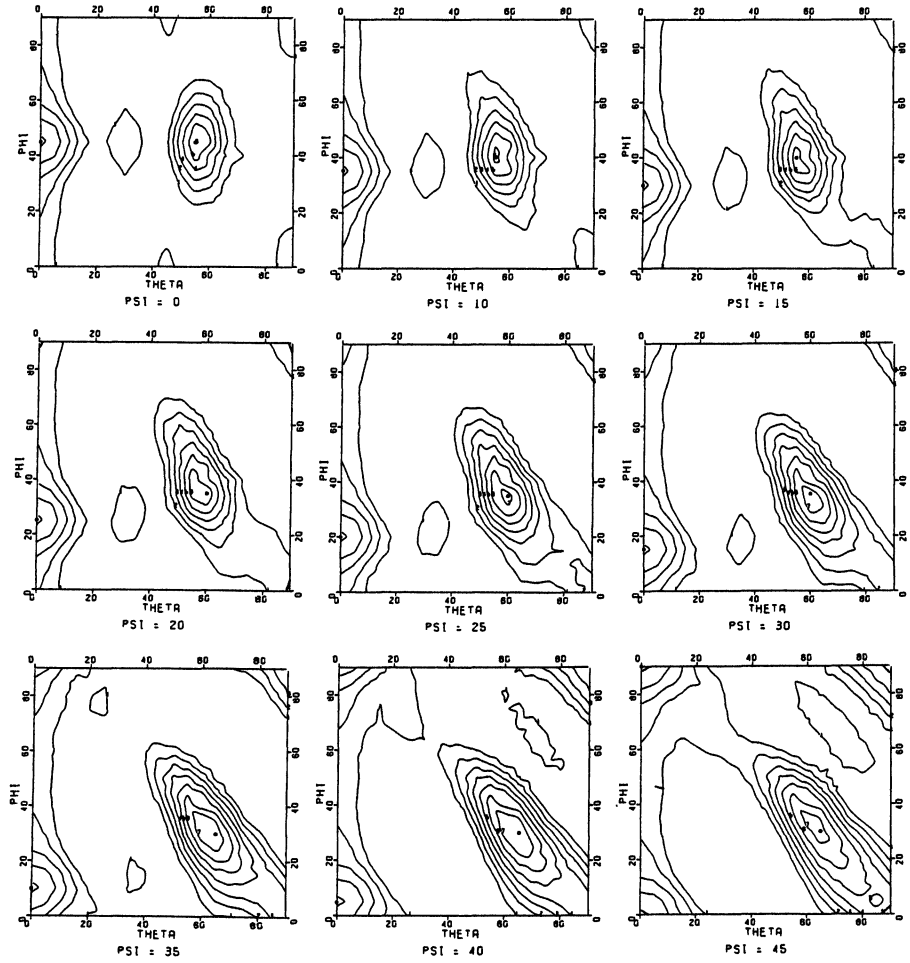

Figure 7. Spatial-orientation distribution of crystallites in the as cold-rolled phosphorus-steel sheet phi (ϕ) vs theta (θ) at constant psi (ψ) sections. Orientation density contours at 1, 2, 3... times random units.

crystallographically equivalent planes, and are located between the $(\bar{1}11)$ fiber and the $(001)[1\bar{1}0]$ components of the cold-rolled texture of the steel sheet. These observations suggest that the minor components B and C of the annealed texture were nucleated in regions between the $(\bar{1}11)$ fiber and the $(001)[1\bar{1}0]$ components of the deformation texture.

The orientation-density variations along the skeleton lines of the annealed textures are shown in Figure 13. The major $(\bar{1}11)$ fiber texture component A has its maximum orientation density at the $(\bar{1}11)[1\bar{1}2]$ and $(\bar{1}11)[\bar{1}\bar{2}1]$ orientations. It is interesting to note that the intensity of these orientations in the cold-rolled texture is at a minimum (compare Figure 13 with Figure 9). Conversely, the orientations that have a maximum intensity in the cold-rolled texture diminish to a minimum intensity in the annealed texture. These results

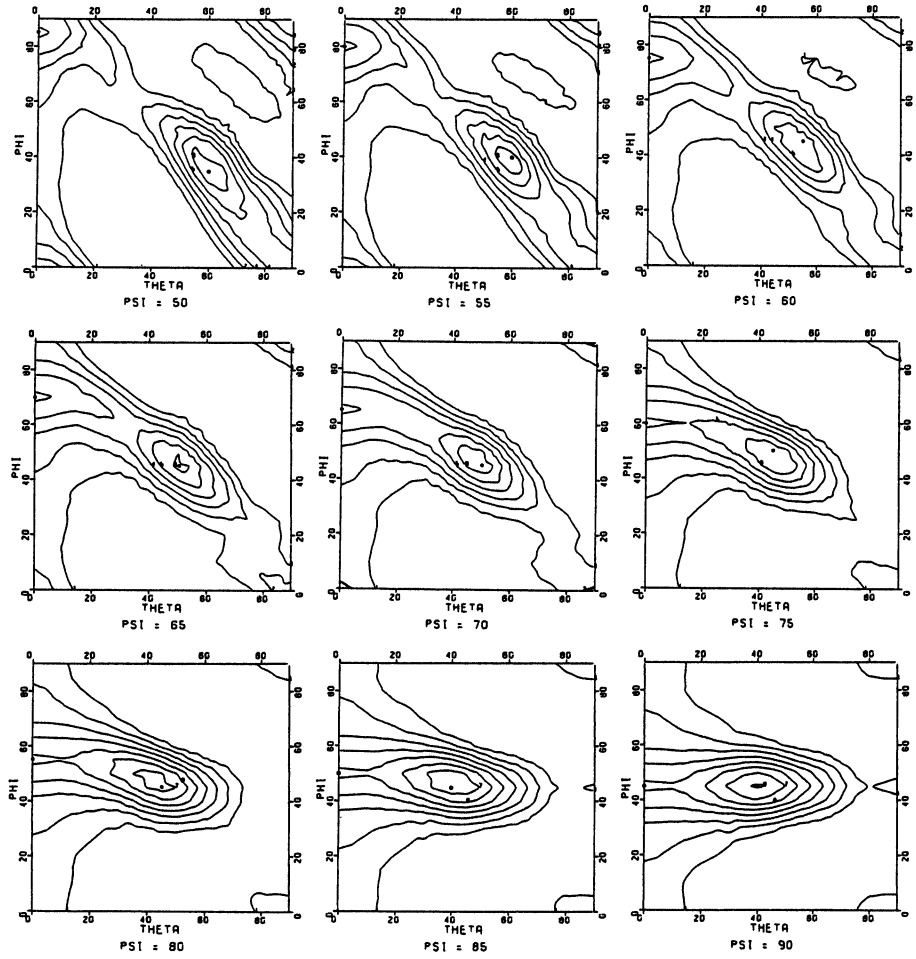

Figure 7. (Continued)

indicate that recrystallized grains are nucleated in regions having orientations in between the major texture components, that is, in regions where a transition of the crystallite orientations from one major texture component to another major component occurs, such as the microband region in between two principal matrix bands.[21] These recrystallized grains then grow at the expense of the matrix. Consequently, the principal components of the cold-rolled texture diminish, and are eventually replaced by a new set of prominent components of the recrystallization texture in the annealed sheet.

The minor texture components B and C differ from each other only slightly in orientation and in intensity. They may be considered as limited fiber components with approximately a <311> axis normal to the rolling plane.

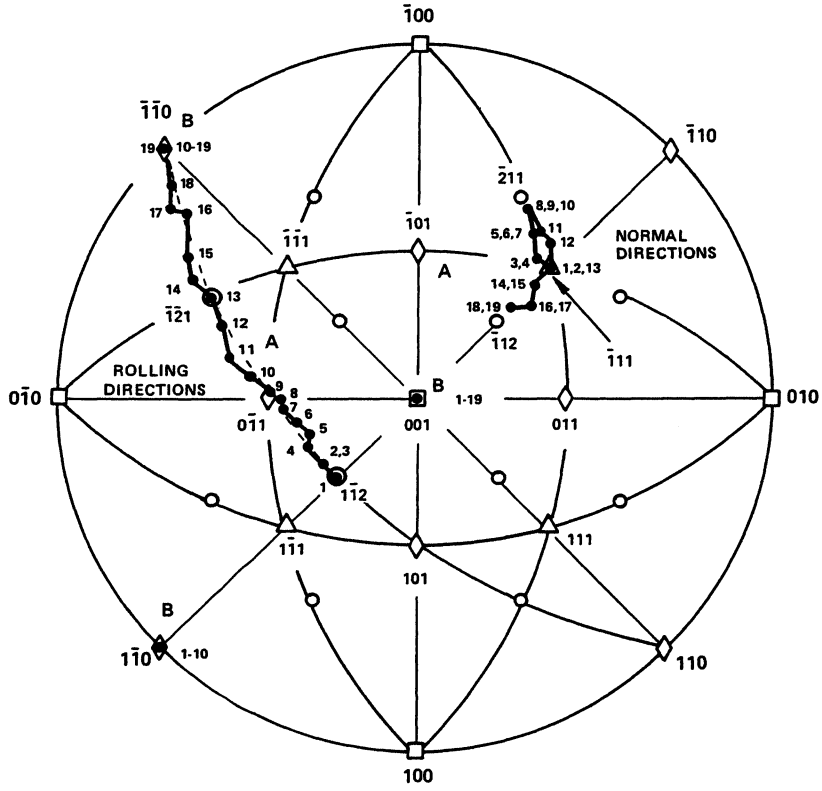

Figure 8. Stereographic projection showing orientation variations along the skeleton lines of components A and B in the as-cold-rolled phosphorus-steel sheet.

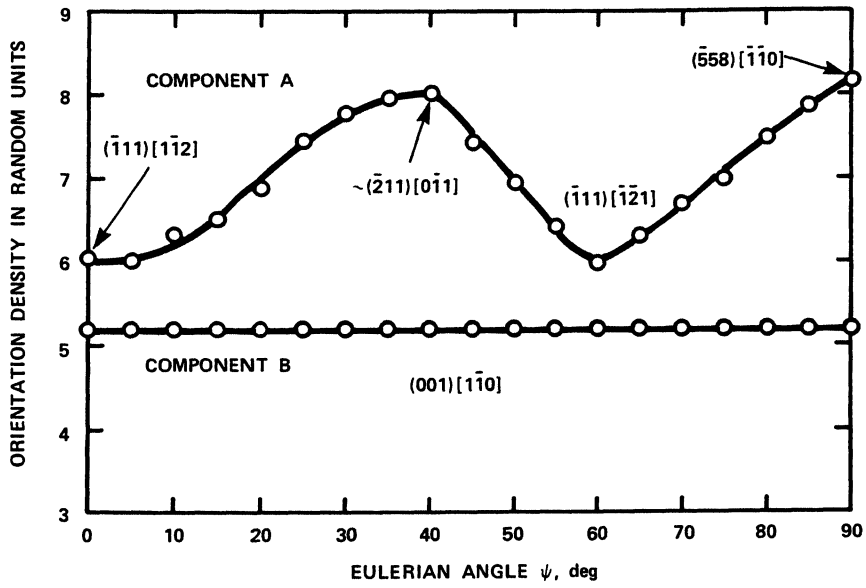

Figure 9. Orientation density variations along the skeleton lines of components A and B in the as-cold-rolled phosphorus-steel sheet.

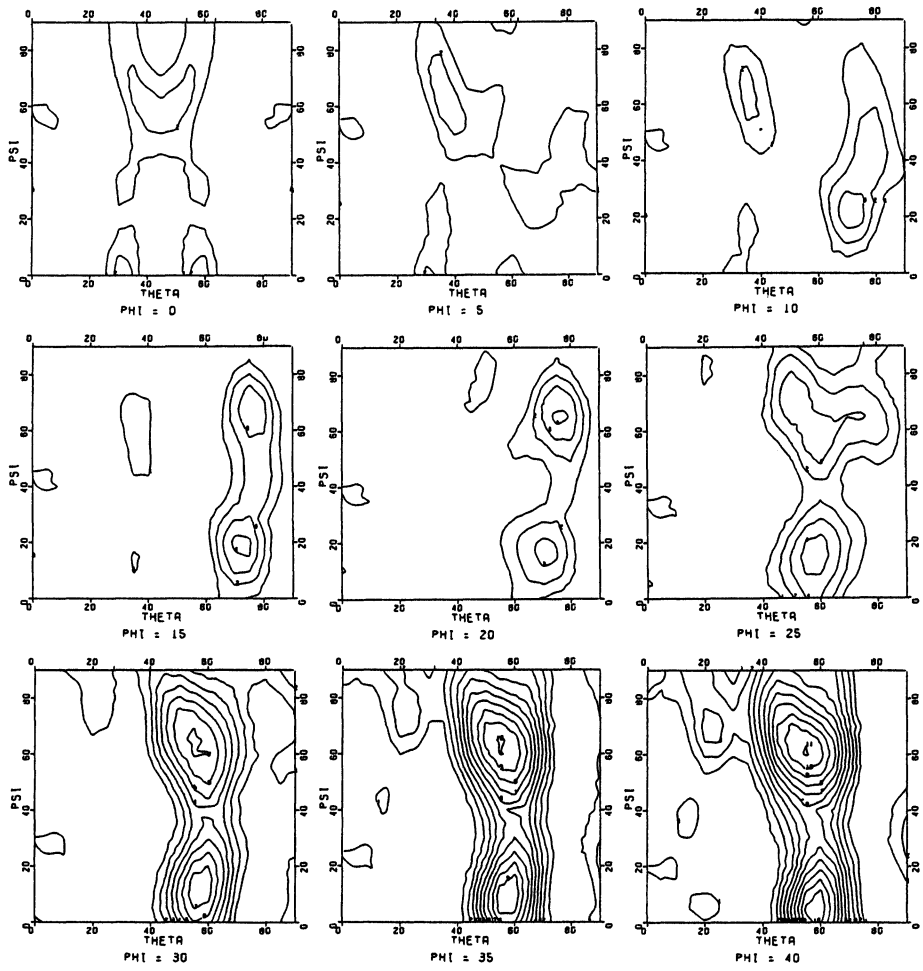

Figure 10. Spatial orientation distribution of crystallites in the annealed phosphorus-steel sheet psi (ψ) vs theta (θ) at constant phi (ϕ) sections. Orientation density contours at 1, 2, 3 ... times random units.

DISCUSSION

The present work constitutes the first extensive study of the spatial-orientation distribution of the crystallites in as-cold-rolled and in annealed low-carbon phosphorus-steel sheets. Similar orientation-distribution studies for aluminum-killed steels were reported by Bunge[22] and by Bunge and Roberts.[23] However, the characteristic variations of the orientation density in the as-cold-rolled and the annealed sheets of the present phosphorus steel (that is, the intensity maximum of the annealed sheet occurs at the intensity minimum of the cold-rolled sheet, and vice versa), were not clearly indicated by the results of Bunge[22] for the aluminum-killed steels. However, in a more recent study by neutron

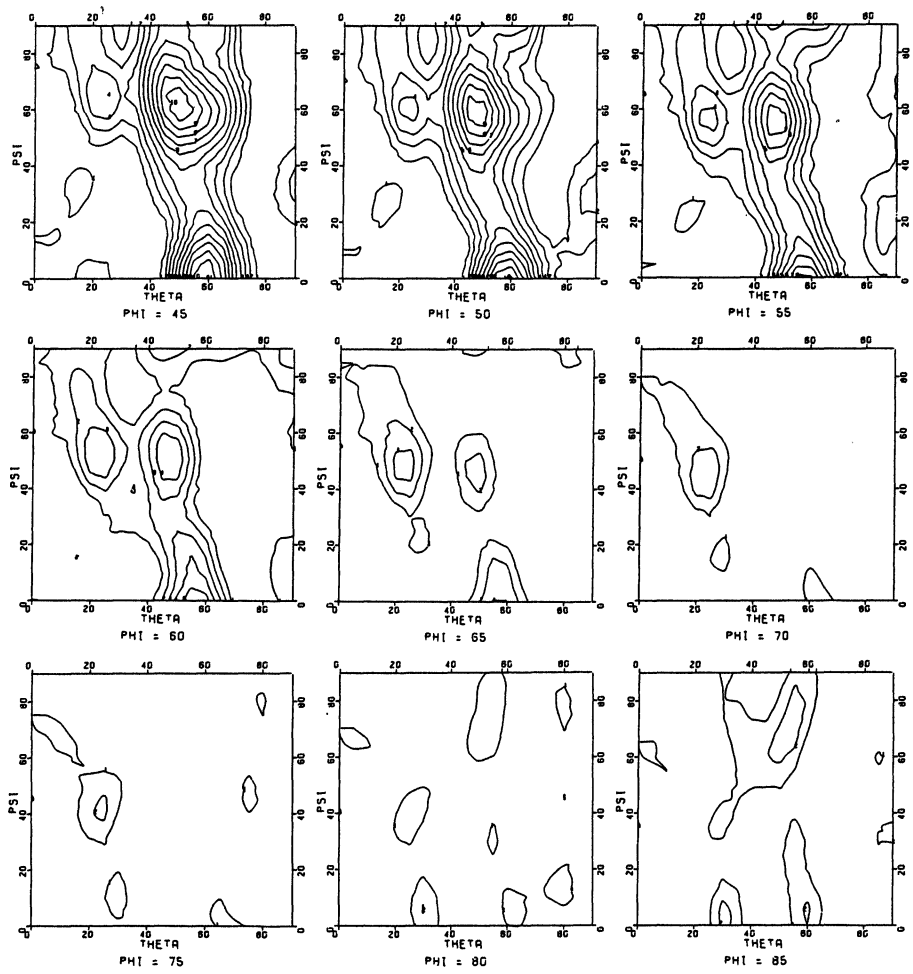

Figure 10. (Continued)

diffraction on the texture development in low-carbon iron or steel, Bunge and co-workers[24,25] have examined the orientation distribution functions of the cold rolling and annealing textures rather extensively. Based on the orientation-density variations along the skeleton lines of the cold rolling and annealing textures (the annealing texture is intermediate between the maximum-density orientations of the deformation texture components), Bunge et al.[25] have come to the same conclusion regarding the origin of the recrystallization texture in their heavily rolled sheets. That is, the recrystallization texture is originated by nucleation in the transition band or microband regions.

As pointed out previously[1-4] the annealing texture of the phosphorus-containing steels is clearly different from that of aluminum-killed steels. The plastic anisotropy parameters, r_m and Δr, of the phosphorus steels are substantially superior (high r_m and low Δr values) to those of the aluminum-killed steels. During recent years, numerous

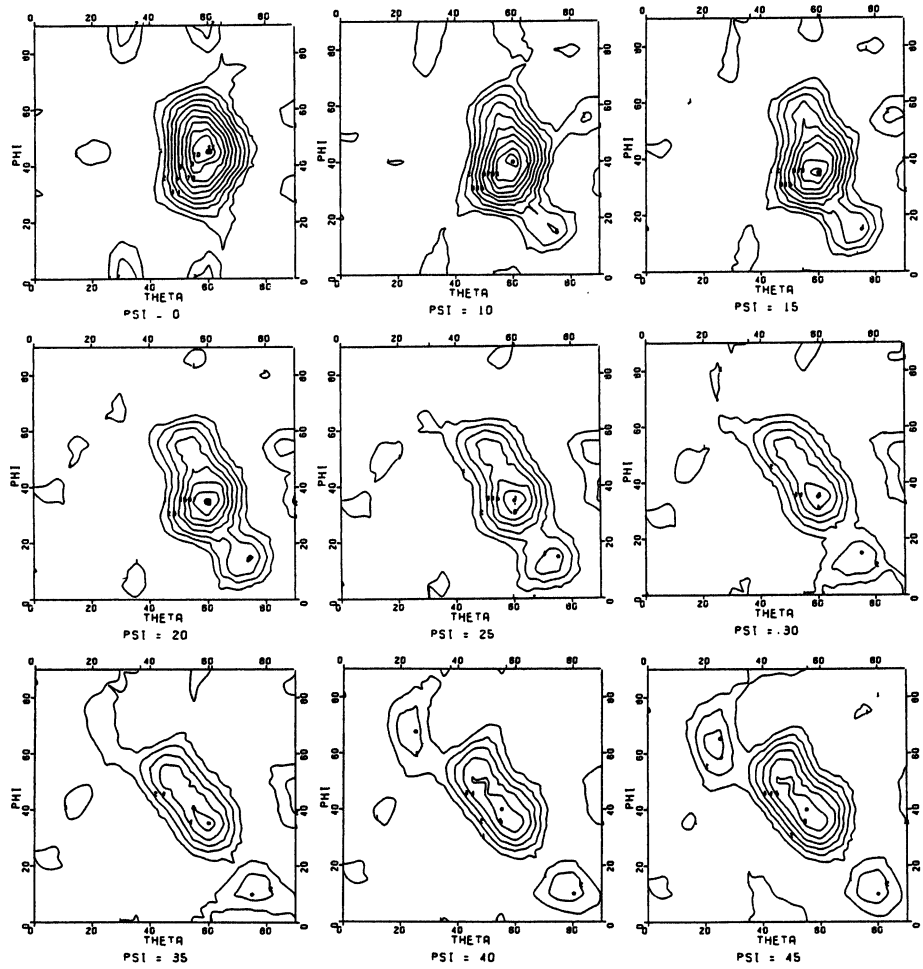

Figure 11. Spatial-orientation distribution of crystallites in the annealed phosphorus-steel sheet phi (ϕ) vs theta (θ) at constant psi (ψ) sections. Orientation density contours at 1, 2, 3 ... times random units.

authors[26-28] have used the crystallite-orientation-distribution analysis to study the textures of various low-carbon deep-drawing or high-strength steels. However, most of these studies consisted of the examination of only the $\phi = 45$ sections of the distribution function for the purpose of identifying the ideal orientations of the textures. A complete examination of the characteristics of the crystallite-orientation distribution of the various steels was not reported.

As is widely recognized by researchers in texture studies, the spatial-orientation-distribution function provides an unambiguous representation of the textures in polycrystalline aggregates. With this orientation-distribution function, the texture of the material is completely and quantitatively represented by the coefficients of the spherical harmonic series, $W_{\ell mn}$. Consequently, one of the most important

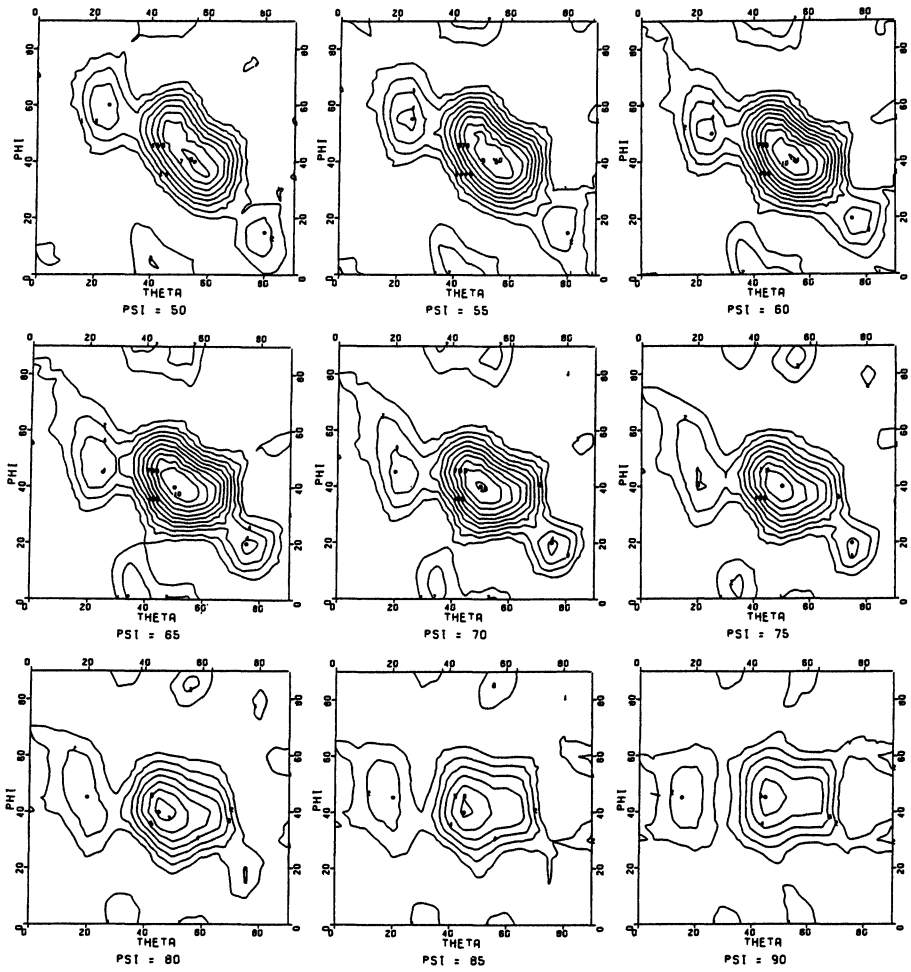

Figure 11. (Continued)

applications of the spatial-orientation-distribution analysis is that all variations in the texture can be accounted for when the physical or mechanical properties of a polycrystalline aggregate are calculated on the basis of the properties of single crystals. By doing this, not only can the properties of textured materials be predicted, but also a basic understanding of how the individual crystallites interact to produce the properties of polycrystalline aggregates can be derived.

The coefficients of the orientation-distribution function, $W_{\ell mn}$, of the as-cold-rolled and the annealed sheets of the present phosphorus steel are provided in Table II and Table III, respectively. With these coefficients, the elastic constants and Young's modulus of these steel sheets can be calculated from the plastic constants for single crystals by incorporating averaging methods proposed by Voigt, Reuss, or Hill, with the texture weighting functions. These results and their comparison with experimental measurements are expected to be presented in a forthcoming paper.

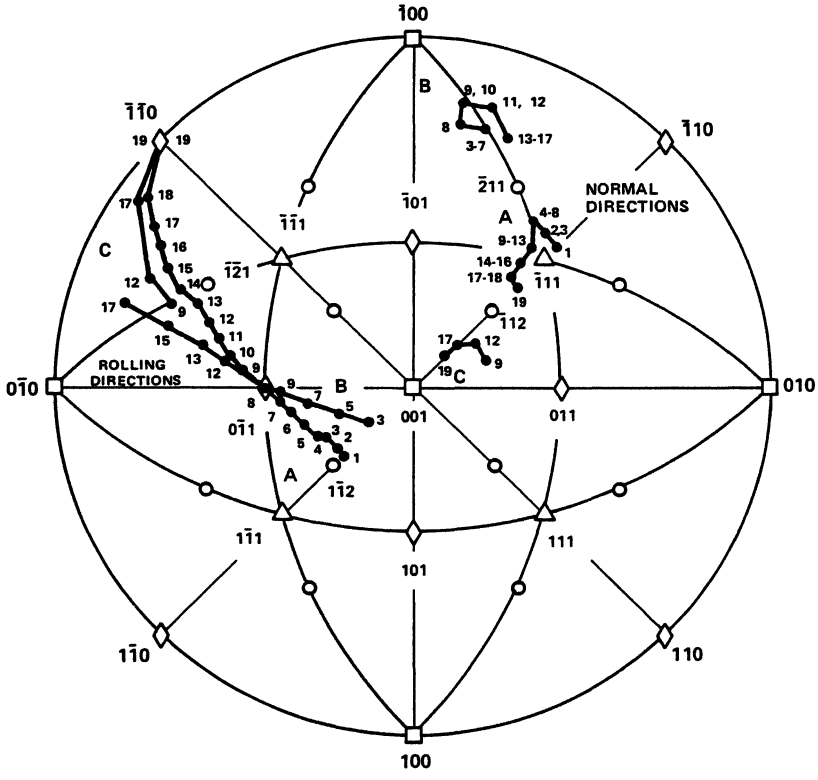

Figure 12. Stereographic projection showing orientation variations along the skeleton lines of components A, B, and C in the annealed phosphorus-steel sheet.

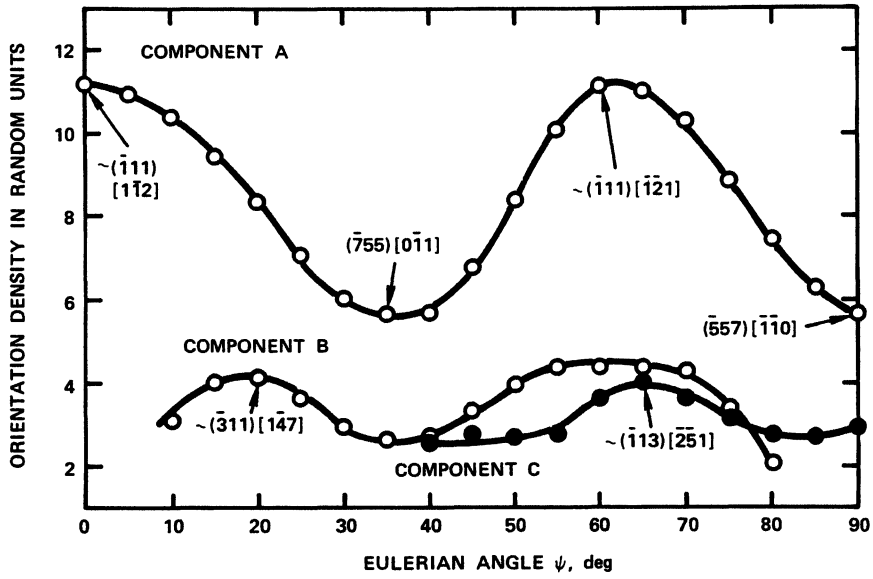

Figure 13. Orientation density variations along the skeleton lines of components A, B, and C in the annealed phosporus-steel sheet.

TABLE II

Coefficients of the Spatial-Orientation-Distribution Function for Crystallites in the As-Cold-Rolled Sheet of Phosphorus Steel

ℓ	m	n	$W_{\ell mn}$	ℓ	m	n	$W_{\ell mn}$
0	0	0	0.017 9112	10	0	4	0.001 0584
					2	4	-0.000 1630
2	0	0	0.000 0000		4	4	0.000 3343
	2	0	0.000 0000		6	4	-0.000 5725
					8	4	0.000 0585
4	0	0	-0.003 3491		10	4	0.000 1756
	2	0	-0.002 4172				
	4	0	-0.005 5361		0	8	0.001 2597
					2	8	-0.000 1940
	0	4	-0.002 0015		4	8	0.000 3978
	2	4	-0.001 4445		6	8	-0.000 6814
	4	4	-0.003 3085		8	8	0.000 0697
					10	8	0.000 2091
6	0	0	0.006 3586				
	2	0	-0.003 5877	12	0	0	0.002 5056
	4	0	0.000 8394		2	0	-0.001 9874
	6	0	-0.000 3027		4	0	0.000 2639
					6	0	-0.000 4101
	0	4	-0.011 8959		8	0	-0.000 8982
	2	4	0.006 7119		10	0	0.000 2520
	4	4	-0.001 5704		12	0	-0.001 1471
	6	4	0.000 5663				
					0	4	-0.001 8016
8	0	0	0.001 5944		2	4	0.001 4403
	2	0	-0.000 3155		4	4	-0.000 8308
	4	0	0.002 9351		6	4	0.000 0951
	6	0	-0.000 5702		8	4	-0.000 7228
	8	0	0.002 2771		10	4	0.000 4133
					12	4	-0.000 4944
	0	4	0.000 5996				
	2	4	-0.000 1186		0	8	0.004 6405
	4	4	0.001 1037		2	8	-0.003 6970
	6	4	-0.000 2144		4	8	0.001 4134
	8	4	0.000 8563		6	8	-0.000 4713
					8	8	0.000 3106
	0	8	0.000 9135		10	8	-0.000 3907
	2	8	-0.000 1808		12	8	-0.000 2217
	4	8	0.001 6817				
	6	8	-0.000 3267		0	12	0.000 4853
	8	8	0.001 3047		2	12	-0.000 3810
					4	12	-0.000 1709
10	0	0	-0.001 0503		6	12	-0.000 1486
	2	0	0.000 1618		8	12	-0.000 6480
	4	0	-0.000 3317		10	12	0.000 2547
	6	0	0.000 5682		12	12	-0.000 6790
	8	0	-0.000 0581				
	10	0	-0.000 1743				

TABLE II (continued)

ℓ	m	n	$W_{\ell mn}$	ℓ	m	n	$W_{\ell mn}$
14	0	0	0.000 8954	16	0	4	0.001 3652
	2	0	-0.000 7318		2	4	-0.001 6840
	4	0	0.000 8084		4	4	0.000 7558
	6	0	-0.000 7398		6	4	-0.000 1764
	8	0	0.000 2853		8	4	0.000 2695
	10	0	-0.000 1949		10	4	0.000 5531
	12	0	-0.000 0920		12	4	0.000 0806
	14	0	0.000 0892		14	4	-0.000 1109
					16	4	0.000 1538
	0	4	-0.000 6585				
	2	4	0.000 5381		0	8	-0.000 8144
	4	4	-0.000 5945		2	8	0.000 9662
	6	4	0.000 5440		4	8	-0.000 4328
	8	4	-0.000 2098		6	8	0.000 2043
	10	4	0.000 1433		8	8	-0.000 0578
	12	4	0.000 0676		10	8	-0.000 2958
	14	4	-0.000 0656		12	8	0.000 0824
					14	8	0.000 0080
	0	8	-0.000 7066		16	8	0.000 1456
	2	8	0.000 5774				
	4	8	-0.000 6379		0	12	-0.001 5391
	6	8	0.000 5838		2	12	0.001 8447
	8	8	-0.000 2251		4	12	-0.000 8268
	10	8	0.000 1538		6	12	0.000 3379
	12	8	0.000 0726		8	12	-0.000 1594
	14	8	-0.000 0704		10	12	-0.000 5756
					12	12	0.000 0922
	0	12	-0.000 8580		14	12	0.000 0435
	2	12	0.000 7011		16	12	0.000 1597
	4	12	-0.000 7746				
	6	12	0.000 7088		0	16	0.000 4474
	8	12	-0.000 2734		2	16	-0.000 5878
	10	12	0.000 1868		4	16	0.000 2646
	12	12	0.000 0881		6	16	0.000 0352
	14	12	-0.000 0855		8	16	0.000 1849
					10	16	0.000 2133
16	0	0	-0.000 2384		12	16	0.000 1489
	2	0	0.000 2089		14	16	-0.000 0910
	4	0	-0.000 0919		16	16	0.000 2733
	6	0	0.000 2511				
	8	0	0.000 1818				
	10	0	-0.000 0207				
	12	0	0.000 2760				
	14	0	-0.000 1099				
	16	0	0.000 5009				

TABLE III

Coefficients of the Spatial-Orientation-Distribution Function for Crystallites in the Annealed Sheet of Phosphorus Steel

ℓ	m	n	$W_{\ell mn}$	ℓ	m	n	$W_{\ell mn}$
0	0	0	0.017 9112	10	0	4	0.004 3103
					2	4	-0.000 4321
2	0	0	0.000 0000		4	4	-0.000 3728
	2	0	0.000 0000		6	4	-0.001 3958
					8	4	0.000 6317
4	0	0	-0.011 5013		10	4	0.000 3463
	2	0	-0.002 9016				
	4	0	-0.000 0346		0	8	0.005 1302
					2	8	-0.000 5143
	0	4	-0.006 8733		4	8	-0.000 4438
	2	4	-0.001 7341		6	8	-0.001 6613
	4	4	-0.000 0207		8	8	0.000 7519
					10	8	0.000 4122
6	0	0	0.006 8518				
	2	0	-0.002 5992	12	0	0	0.001 2701
	4	0	0.000 4716		2	0	-0.002 9816
	6	0	0.001 6528		4	0	0.001 5465
					6	0	-0.000 3209
	0	4	-0.012 8186		8	0	-0.000 1794
	2	4	0.004 8626		10	0	-0.000 4689
	4	4	-0.000 8823		12	0	0.000 2812
	6	4	-0.003 0922				
					0	4	-0.003 1154
8	0	0	0.002 1202		2	4	0.001 2344
	2	0	0.001 8995		4	4	-0.000 4774
	4	0	-0.001 6750		6	4	-0.000 3131
	6	0	0.003 3327		8	4	0.000 2264
	8	0	-0.000 5599		10	4	-0.000 4385
					12	4	-0.000 2175
	0	4	0.000 7973				
	2	4	0.000 7143		0	8	0.005 5287
	4	4	-0.000 6299		2	8	-0.004 2102
	6	4	0.001 2533		4	8	0.001 9488
	8	4	-0.000 2105		6	8	0.001 1901
					8	8	-0.000 4728
	0	8	0.001 2148		10	8	0.000 2504
	2	8	0.001 0884		12	8	0.000 5428
	4	8	-0.000 9597				
	6	8	0.001 9095		0	12	-0.000 5166
	8	8	-0.000 3208		2	12	-0.000 8925
					4	12	0.000 5193
10	0	0	-0.004 2775		6	12	-0.000 2505
	2	0	0.000 4288		8	12	-0.000 0010
	4	0	0.000 3700		10	12	-0.000 3595
	6	0	0.001 3852		12	12	0.000 0492
	8	0	-0.000 6269				
	10	0	-0.000 3437				

TABLE III (Continued)

ℓ	m	n	$W_{\ell mn}$	ℓ	m	n	$W_{\ell mn}$
14	0	0	0.000 9998	16	0	4	-0.003 6953
	2	0	0.000 2637		2	4	-0.002 0779
	4	0	-0.000 8407		4	4	0.000 4759
	6	0	0.000 3505		6	4	0.001 8922
	8	0	-0.000 6096		8	4	0.000 3091
	10	0	0.000 0749		10	4	0.000 8489
	12	0	0.000 3345		12	4	-0.000 8568
	14	0	-0.000 0902		14	4	-0.000 2720
					16	4	-0.000 0411
	0	4	-0.000 7352				
	2	4	-0.000 1939		0	8	0.001 5934
	4	4	0.000 6182		2	8	0.001 5297
	6	4	-0.000 2577		4	8	-0.000 3402
	8	4	0.000 4483		6	8	-0.000 9556
	10	4	-0.000 0551		8	8	-0.000 2398
	12	4	-0.000 2460		10	8	-0.000 5098
	14	4	0.000 0664		12	8	0.000 6601
					14	8	0.000 0796
	0	8	-0.000 7890		16	8	0.000 0025
	2	8	-0.000 2081				
	4	8	0.000 6634		0	12	0.003 3086
	6	8	-0.000 2766		2	12	0.002 7498
	8	8	0.000 4811		4	12	-0.000 6156
	10	8	-0.000 0591		6	12	-0.001 8903
	12	8	-0.000 2640		8	12	-0.000 4262
	14	8	0.000 0712		10	12	-0.000 9618
					12	12	0.001 1750
	0	12	-0.000 9580		14	12	0.000 1907
	2	12	-0.000 2527		16	12	0.000 0154
	4	12	0.000 8055				
	6	12	-0.000 3358		0	16	-0.001 7846
	8	12	0.000 5841		2	16	-0.000 4085
	10	12	-0.000 0718		4	16	0.000 1031
	12	12	-0.000 3205		6	16	0.000 7826
	14	12	0.000 0865		8	16	0.000 0492
					10	16	0.000 2749
16	0	0	-0.000 7132		12	16	-0.000 1409
	2	0	0.001 0080		14	16	-0.000 1667
	4	0	-0.000 2084		16	16	-0.000 0342
	6	0	0.000 0546				
	8	0	-0.000 1772				
	10	0	-0.000 1559				
	12	0	0.000 4809				
	14	0	-0.000 1362				
	16	0	-0.000 0419				

SUMMARY

By using the generalized spherical harmonics technique, the crystallite-orientation-distribution functions for as-cold-rolled and for annealed sheets of a deep-drawing phosphorus steel were determined. These crystallite-orientation-distribution functions were mainly characterized by high-density clusters along an oval-shaped cross-sectioned tube running roughly parallel to the ψ-axis in the Eulerian space. The textures of both the as-cold-rolled and the annealed sheets could be described approximately as a [111] fiber with the fiber axis being normal to the plane of the sheet.

For the as-cold-rolled sheet, the intensity or orientation-density maxima were at approximately $(\bar{2}11)[0\bar{1}1]$ and $(\bar{5}58)[1\bar{1}0]$, and the intensity minima at $(\bar{1}11)[1\bar{1}2]$ and $(\bar{1}11)[\bar{1}21]$. For the annealed sheet this orientation-density distribution was approximately reversed, that is, the intensity maxima were at approximately $(\bar{1}11)[1\bar{1}2]$ and $(\bar{1}11)[\bar{1}21]$ and the intensity minima at $(\bar{7}55)[0\bar{1}1]$ and $(\bar{5}57)[1\bar{1}0]$. The latter two orientations are so close to $(\bar{2}11)[0\bar{1}1]$ and $(\bar{5}58)[1\bar{1}0]$ that they may be considered the same. These features were discussed in terms of nucleation and growth mechanisms in recrystallization. The crystallite orientation distribution in the annealed sheet of the present phosphorus steel is clearly different from that of annealed sheet of deep-drawing aluminum-killed steel.

The numerical coefficients of the orientation-distribution functions of the as-cold-rolled and the annealed sheets of the present deep-drawing phosphorus steel were provided. These coefficients, which represent a complete description of the textures of the sheets, can be used in conjunction with texture weighting functions to calculate physical or mechanical properties of the sheets from the properties of single crystals.

ACKNOWLEDGMENT

The author wishes to express his sincere appreciation to P. R. Morris of Armco, Inc., who made his original computer program for crystallite orientation-distribution analysis available to us, and to R. W. Whitmore of this laboratory, who converted the original program to work successfully in our CDC-6500 computer system. Without their expert cooperation, the present study would not have been accomplished. The competent assistance of R. E. Stecik and P. E. Toohill in conducting various experimental measurements is sincerely acknowledged.

REFERENCES

1. H. Hu, *Texture Cryst. Sol.*, 2, 113 (1976).
2. H. Hu, *Met. Trans.*, 8A, 1567 (1977).
3. H. Hu, *Texture Cryst. Sol.*, 3, 215-230 (1979).
4. H. Hu, in *Formable HSLA and Dual-Phase Steels*, ed. A. T. Davenport, (TMS-AIME Conference Proceedings, 1979), p. 109.

5. H. Hu, "Low-Carbon Phosphorus Steels for High Strength Cold-Rolled Sheet Applications," Unpublished work, U.S. Steel Research Laboratory.
6. R. J. Roe, *J. Appl. Phys.*, 36, 2024 (1965).
7. R. J. Roe, *J. Appl. Phys.*, 37, 2069 (1966).
8. H. J. Bunge, *Zeit. Metallk.*, 56, 872 (1965).
9. H. J. Bunge, *Mathematische Methoden der Texturanalyse*, (Akademie-Verlag, Berlin, 1969).
10. P. R. Morris and A. J. Heckler, *Advances in X-Ray Analysis*, 1968, Vol. 11, p. 454.
11. E. S. Meieran, *Rev. Sci. Instr.*, 33, 319 (1962).
12. S. L. Lopata and E. B. Kula, *Trans. TMS-AIME*, 224, 865 (1962).
13. S. Leber, *Rev. Sci. Instr.*, 36, 1747 (1965).
14. J. A. Elias and A. J. Heckler, *Trans. TMS-AIME*, 239, 1237 (1967).
15. L. G. Schulz, *J. Appl. Phys.*, 20, 1030 (1949).
16. P. R. Morris, *Texture Cryst. Sol.*, 2, 57 (1976).
17. J. Jura and J. Pospiech, *Texture Cryst. Sol.*, 2, 81 (1976).
18. H. J. Bunge, J. Tobisch, and A. Mucklich, *Texture*, 1, 211 (1974).
19. M. Humbert, F. Wagner, and R. Baro, *Texture Cryst. Sol.*, 3, 27 (1978).
20. G. J. Davies, D. J. Goodwill, and J. S. Kallend, *J. Appl. Cryst.*, 4, 67 (1971).
21. H. Hu, in *Recovery and Recrystallization of Metals*, (Interscience Publishers, New York, 1963), p. 311.
22. H. J. Bunge, *Phys. Stat. Sol.*, 26, 167 (1968).
23. H. J. Bunge and W. T. Roberts, *J. Appl. Cryst.*, 2, 116 (1969).
24. D. Schläfer and H. J. Bunge, *Texture*, 1, 157 (1974).
25. H. J. Bunge, D. Schleusener, and D. Schläfer, *Met. Sci. J.*, 8, 413 (1974).
26. A. J. Heckler and W. G. Granzow, *Met. Trans.*, 1, 2089 (1970).
27. H. Inagaki and T. Suda, *Texture*, 1, 129 (1973).
28. D. J. Willis and M. Hatherly, in *Texture and Properties of Materials*, 4th Int. Conf. on Texture, Cambridge, (The Metals Society, 1976), p. 48.